Mar Biol (2016) 163:110
DOI 10.1007/s00227-016-2891-1

ORIGINAL PAPER

# Spatial distribution of phlorotannins and its relationship with photosynthetic UV tolerance and allocation of storage carbohydrates in blades of the kelp *Lessonia spicata*

**Iván Gómez[1,2] · Sonia Español[1,3] · Karina Véliz[1,4,5] · Pirjo Huovinen[1,2]**

Received: 29 January 2016 / Accepted: 8 April 2016 / Published online: 21 April 2016


**Abstract** The action of an intercalary meristem in the fronds determines the growth patterns of the sub-Antarctic kelp *Lessonia spicata*, which result in gradients in physiological activity and tissue composition. In this study, the allocation of phenolic compounds (phlorotannins) was examined in relation with the longitudinal patterns of photosynthesis (as $^{14}C$ fixation and chlorophyll fluorescence) and storage of carbohydrates (mannitol and laminaran) in the blades. Moreover, exposures to UV radiation were carried out in order to test the photoprotective role of phlorotannins along different blade regions. The content of soluble phlorotannins was higher in the basal regions than in the middle and apical parts, which was correlated with the longitudinal allocation of mannitol and light-independent $^{14}C$ fixation, two indicators of growth activity. In contrast, photosynthetic $^{14}C$ fixation and allocation of laminaran were inversely related to the levels of phlorotannins along the blade. The photosynthetic characteristics measured using Imaging-PAM fluorescence did not show clear intra-blade patterns. UV exposures resulted in a decline in chlorophyll fluorescence ($F_v/F_m$) after 24 and 48 h (10 and 20 % respectively); however, no differential effects in different regions of the fronds were observed. The content of soluble phlorotannins in response to UV radiation was mostly determined by the time of exposure and less by the blade region: After a 6-h exposure phlorotannins decreased around 40 %, while after 48 h UV radiation stimulated the synthesis of phlorotannins by 22–99 %. Overall, after a 12-h UV exposure an increasing tendency of phlorotannins allocated in the basal regions of the blade was demonstrated. This study reinforces the idea that phlorotannins are important not only as secondary metabolites, but also their allocation in the thallus of kelps is integrated within the morpho-functional characteristics related to photosynthesis and biomass formation.

Responsible Editor: F. Weinberger.

Reviewed by Undisclosed experts.

**Electronic supplementary material** The online version of this article (doi:10.1007/s00227-016-2891-1) contains supplementary material, which is available to authorized users.

✉ Iván Gómez
igomezo@uach.cl

[1] Instituto de Ciencias Marinas y Limnológicas, Universidad Austral de Chile, Valdivia, Chile

[2] Centro Fondap de Investigación en Dinámica de Ecosistemas de Altas Latitudes (IDEAL), Valdivia, Chile

[3] Programa de Doctorado en Biología Marina, Universidad Austral de Chile, Valdivia, Chile

[4] Programa de Doctorado en Biología y Ecología Aplicada (BEA), Universidad Católica del Norte, Coquimbo, Chile

[5] Present Address: Departmento de Biología Marina, Facultad de Ciencias del Mar, Universidad Católica del Norte, Coquimbo, Chile

## Introduction

Large macroalgae of the order Laminariales (also denominated "kelps") are characterized by complex morpho-functional processes, which are strongly determined by the action of an intercalary meristem (Küppers and Kremer 1978). During the growth phase, the blade is elongated from this meristem resulting in a longitudinal arrangement of zones with different development, age and metabolic activity, i.e., a gradient of tissues with different ontogenetic stages (Kogame and Kawai 1996). This spatial configuration has not only consequences for metabolism but also

determines a suite of biomechanical properties of these algae (Krumhansl et al. 2015). In general, apical zones of kelps are regions of carbon assimilation via photosynthesis, while the basal regions of the blade serve as carbon sink to power anabolic processes. In fact, reserve carbohydrates (e.g., laminaran) synthesized during summer are translocated passively as low-weight sugars (e.g., mannitol) or amino acids to the meristem, where they are transformed to, e.g., pyruvate to power the energy requirements during active growth in winter–spring (Schmitz 1981; Gómez and Huovinen 2012).

Light-independent carbon fixation (LICF) via carboxylating enzymes is the pathway involved in the capacity of these algae to savage $CO_2$ lost in glycolysis of translocated carbohydrates (Kremer 1984). In most kelps, both LICF and photosynthetic carbon fixation via RuBisCo are seasonally synchronized, which represents the physiological basis of the growth patterns of these organisms (Lüning et al. 1973; Chapman and Craigie 1978). Because of this, high-latitude seaweeds have exploited very efficiently the potential for LICF as a strategy to minimize the carbon losses due to high respiration and to optimize the supply of carbon skeletons during rapid growth in the short open-water season (Drew and Hastings 1992; Gómez and Wiencke 1998; Wiencke et al. 2009). However, temperate species, which grow during the spring/summer season, show also high LICF rates in basal thallus regions (Cabello-Pasini and Alberte 1997; Gómez et al. 2007).

It was proposed recently that the morpho-functional patterns related to thallus elongation and light carbon fixation mechanisms displayed by kelps are important components of UV stress tolerance as carboxylation via RuBisCo is more affected by UV radiation than LICF (Gómez et al. 2007). Thus, the intra-thallus patterns of allocation of organic matter can also be essential to supply the necessary precursors for photoprotective compounds, which show also longitudinal gradients in kelps (Van Alstyne et al. 1999; Connan et al. 2006). In this context, the importance of phlorotannins (polymers of phloroglucinol; 1,3,5-trihydroxybenzene; Ragan and Glombitza 1986) has been emphasized in the last few years. Commonly associated with antiherbivory defense (Targett and Arnold 1998; Jormalainen and Honkanen 2008) and antifouling activity (Wikström and Pavia 2004), phlorotannins have UV-absorbing properties and thus show a UV-shielding function in various kelp species (Pavia et al. 1997; Swanson and Druehl 2002; Swanson and Fox 2007; Huovinen et al. 2010). In fact, UV-mediated increases in phlorotannins can minimize photodamage of photosynthesis and DNA in kelps (Gómez and Huovinen 2010). Recently, high levels of phlorotannins have been correlated with enhanced ROS scavenging activity in intertidal kelps exposed to high UV doses and metals suggesting that these compounds represent primary metabolic antistress agents (Huovinen et al. 2010; Cruces et al. 2012). Their contents in different thallus parts appear to indicate that these compounds are differentially allocated as has been reported for *Saccharina latissima* and *Laminaria digitata*, where high concentrations in reproductive tissues are correlated with enhanced antioxidant capacity (Gruber et al. 2011; Holzinger et al. 2011). Up to now the most important evidence that phlorotannins are related to biomass allocation comes from the fact that they are essential during the formation of cell wall, i.e., phlorotannins are primary compounds and their synthesis can also be triggered by intrinsic algal processes, e.g., cell division and growth (Schoenwaelder 2002; Arnold 2003). However, the question whether phlorotannins in brown algae vary in relation to frond development and how this will affect further patterns in biomass/energy allocation remains open. In higher plants, diverse studies have revealed that differential allocation of phenolic compounds between tissues during leaf development strongly affects the spatial patterns in physiological performance and stress tolerance (e.g., against UV radiation) (Wyka et al. 2008; Meyer et al. 2009; Klem et al. 2012).

In the present study, using a variety of biochemical and photochemical approaches we tested the hypothesis that longitudinal profiles in phlorotannin contents in blades of *Lessonia spicata* (formerly *L. nigrescens*; González et al. 2012) are related to the intrinsic variation in photosynthesis (measured as carbon fixation, chlorophyll fluorescence and reserve carbohydrate contents). Two predictions were examined: a) Due to their fate as primary compounds during growth, the highest contents of phlorotannins are detected in the meristematic basal region and thus correlated with the light-independent carbon fixation (LICF) and storage carbohydrates, and b) due to their role as UV-absorbing compounds, the frond regions allocating higher concentrations of phlorotannins (e.g., the basal parts) are more photoprotected against UV radiation. The model organism, *Lessonia spicata*, was chosen due to its well-known morpho-functional patterns that include rapid phlorotannins induction in response to different environmental factors (Gómez et al. 2007; Gómez and Huovinen 2010; Huovinen et al. 2010; Cruces et al. 2012). Thus, the present study provides unprecedented insights into the spatial variability in key physiological processes and their responses to UV radiation with important implications for growth and primary productivity.

## Materials and methods

### Algal material

Four individuals of *Lessonia spicata* (Suhr) Santelices (Laminariales, Lessoniaceae) were collected in spring

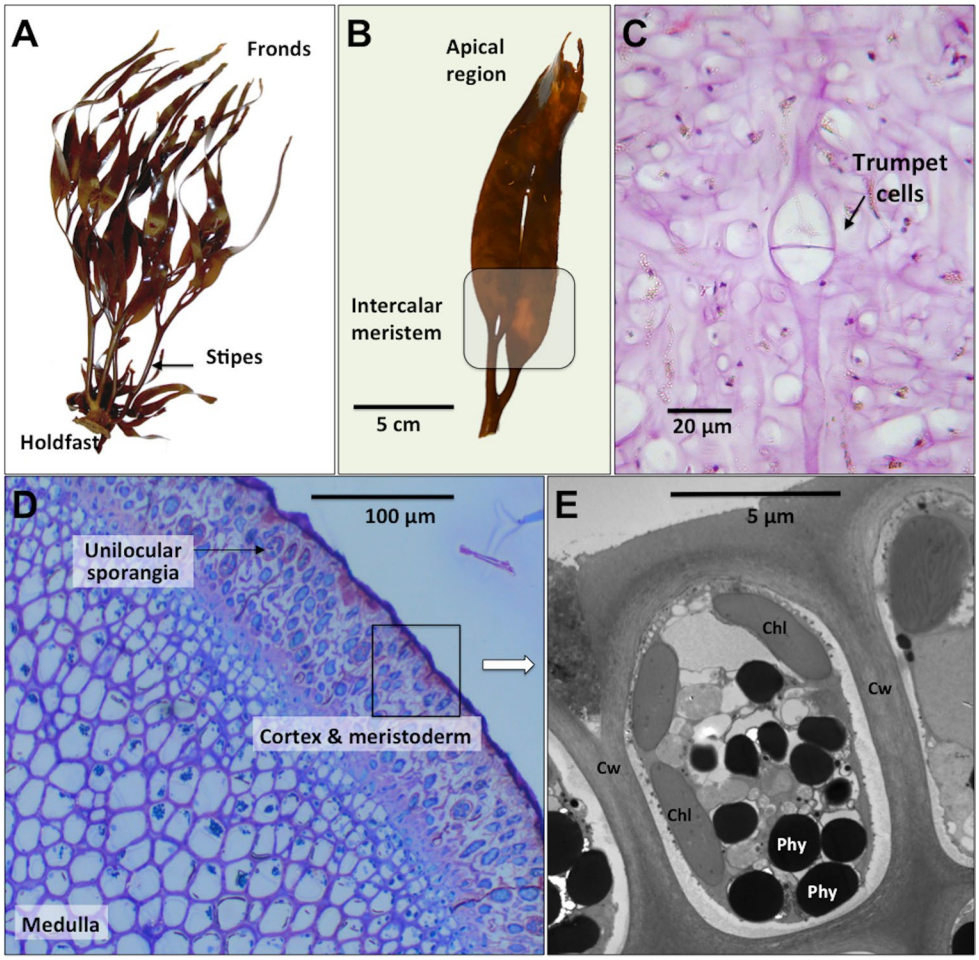


**Fig. 1** Morphology and ultrastructure of *Lessonia spicata*. **a** Different structural parts of an adult sporophyte, **b** a blade indicating the intercalary meristem, **c** medulla with details of medullar "trumpet cells" connected by their swollen ends, **d** cross section of a blade (stained with hematoxiline–eosine and toluidine blue) indicating medulla, cortex, epidermal meristoderm with unilocular sporangia, **e** TEM image of epidermal cells showing large physodes (Phy) containing abundant phlorotannins. Other structures: chloroplasts (Chl), cell wall (Cw)

from the rocky shores of Curiñanco, 25 km from Valdivia, Chile (39°46′S; 73°24′W). The algae were transported to the laboratory where they were cleaned of epiphytes and maintained overnight under constant PAR illumination provided by fluorescent lamps (70 µmol $m^{-2}$ $s^{-1}$, TL Phillips) to allow acclimation to laboratory conditions (13–15 °C; 34 PSU; and vigorous aeration). After 24-h acclimation, four blades from each individual were incubated in aquaria containing 5 L of filtered seawater (0.45 µm, MFS GC50, Japan) in a thermo-regulated water bath according to the methodology described by Gómez et al. (2005).

### Histological determinations: blade architecture and ultrastructure

Internal anatomy and fine structure of different blade parts were examined under light microscopy from samples stained with hematoxiline–eosine and toluidine blue. The ultrastructural localization of phlorotannins in the cells (physodes) of basal blade regions was investigated by transmission electron microscopy (TEM) (Philips 300, the Netherlands). Samples of approximately 3 mm in length were fixed in filtered seawater (0.22 µm), glutaraldehyde (3 % v/v), p-formaldehyde (1 %) and caffeine (0.1 %). After washing with filtered seawater, samples were post-fixed in 2 % osmium tetroxide and 1 % potassium ferricyanide, dehydrated through an ethanol series (10–100 %) and embedded in Spurr resin for 1 week. For staining, 4 % uranyl acetate and lead citrate were used. Samples were observed in a microscope Tecnai 12 (Philips, Holland), operated at 60 kV.

The blades of *Lessonia* are formed by an intercalary meristem, which determines the subsequent division from independent bifurcation (Fig. 1b). When algae reach a critical size, the intercalary bifurcations become less frequent and the fronds grow into an elongate form. Thus, the basal part of the blades is formed by new cells in active growth phase, while the apical parts of the fronds are senescent, generating gradients in metabolic activity (e.g., carbon fixation).

The inner organization of the blade of *L. spicata* is characterized by an epidermal meristematic zone, cortex and medulla. In the medulla, it is possible to observe longitudinally arranged trumpet cells with transport function, which

are forming a complex with hyphae (Fig. 1c). In general, this basic pattern is retained in the different thallus regions. However, in actively growing blades, medullar zone and cortex are more developed in comparison with inactive fronds. Intracellular accumulation of phlorotannins was imaged using toluidine blue (Fig. 1d). Based on TEM analysis these high intracellular concentrations within vegetative cortical cells and unilocular sporangia were confirmed by the presence of large and numerous physodes (Fig. 1e).

### Characterization of longitudinal profiles

Several individual blades with bifurcations, evidence of the action of the intercalary meristem, were selected for the distinct analyses (determination of storage carbohydrates, $^{14}C$ fixation and phlorotannins contents). Sample disks with a diameter of 1 cm were punched from different blade regions (from basal to apical zones) with a cork borer. The algal fragment considered the whole transversal section, including epidermis, cortex and medulla. The sample disks were incubated in Petri dishes (52 disks in each treatment) containing 150 mL of filtered seawater (0.45 µm, MFS GC50, Japan) in a thermo-regulated water bath (13–15 °C) under vigorous aeration.

### Imaging analysis

In vivo Imaging-PAM fluorescence along blades of *L. spicata* was detected using a CCD camera (IMAG-K, Walz, Germany) mounted on a supporting IMAG-MAX/GS box. Along the blades, different measuring regions were defined (see Fig. 2) where fluorescence kinetics such as maximum quantum yield ($\Phi_{PSII}$) and maximum fluorescence of illuminated samples ($F_{m'}$) were determined. In the case of non-photochemical quenching (NPQ), measurements were run in dark-adapted algae (10–15 min) after an excitation pulse with intensity 2400 µmol $m^{-2}$ $s^{-1}$ and 0.8-s duration from a 470-nm LED array (IMAG-MAX/L). The fluorescence output from different regions of each blade was then imaged according a color code ranging between 0 and 1.

In parallel with fluorescence yield measurements, rapid light curves (P–I) based on electron transport rate (ETR) were run along the blades under a gradient of PAR irradiances (0–701 µmol photon $m^{-2}$ $s^{-1}$). The relative electron transport rate (ETR) was estimated relating the effective quantum yield ($\Phi_{PSII}$) and the intensity of actinic radiation (Schreiber et al. 1994), as follows:

$$ETR = \Phi_{PSII} \times E_{PAR} \times FII \times A$$

where $E_{PAR}$ is the incident actinic irradiance. For the fraction of absorbed quanta to PSII (FII), the value of 0.8 corresponding to brown algae (Grzymski et al. 1997) was used.

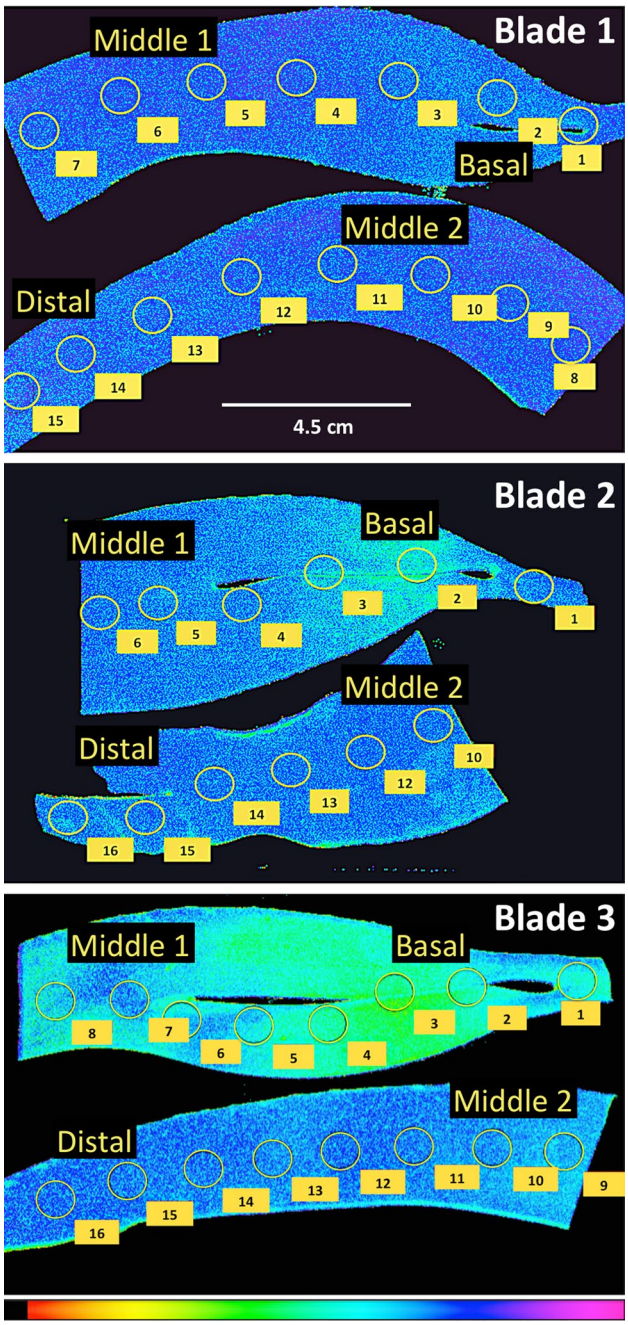


**Fig. 2** Examples of blades of *Lessonia spicata* used for measuring Imaging-PAM fluorescence kinetics. *Circles* and *numbers* in the blades indicate the points of measurements of chlorophyll fluorescence yield and electron transport rate (ETR) versus light (P–E) curves. *Colors* indicate the heterogeneity in a gradient between 0 and 1

The thallus absorptance ($A$) was determined by placing the algae on a cosine-corrected PAR sensor (Licor 192 SB, Lincoln, USA) and calculating the light transmission as:

$$A = 1 - T - R$$

where $T$ is the transmittance (light transmitted throughout the sample $= E_t/E_0$) and R is the reflectance (reflected fraction). It must be noted that absorptance values did not significantly varied along the blades with values around 0.8.

### $^{14}$C fixation

For the measurement of photosynthetic assimilation of $^{14}$C, the disks were incubated in a transparent vial for 30 min at saturating PAR irradiances (250 µmol $m^{-2}$ $s^{-1}$) provided by a halogen lamp mounted in a slide projector (150 W, Reflecta, Germany). In parallel, samples maintained in the dark for 30 min were used to determine the light-independent carbon fixation. The samples were incubated with 0.7 µCi $^{14}$C $mL^{-1}$ as $NaH^{14}CO_3$ (PerkinElmer Inc., USA) and further treated as described by Gómez et al. (2007). The radiation conditions during the measurements were monitored using a Licor 1400 datalogger fitted to a Li 190-S quantum sensor (Li-Cor Inc., USA).

### Determination of storage carbohydrates

Laminaran was extracted by incubating 10–20 mg dry material in 1 mL ethanol (20 %) at 75 °C for 3 h. The extract was then centrifuged at 4000×$g$ for 15 min. Aliquots of 0.5 mL from the supernatant were hydrolyzed with 1 N HCL for 1 h at 100 °C. After neutralization with 1 mL 1 N NaOH, 40 µL of extract was incubated in a solution containing amyloglucosidase (Sigma-Aldrich) buffered with citrate (pH 4.6) at 55 °C for 45 min. After dilution with 350 µL triethanolamine (pH 7.6), 35 µL ATP, 35 µL NADP and 440 µL double-distilled water, the extinction ($Ext_1$) was read in a scanning SUV-2120 spectrophotometer (Scinco, Korea) at a wavelength of 340 nm. Finally, 10 µL of a hexokinase and glucose-6-P-dehydrogenase cocktail (Sigma) was added, and after incubation for 15 min at ambient temperature, a second absorbance ($Ext_2$) was measured at 340 nm. The laminaran content was then determined using the following formula:

$$(\mathrm{Ext}_2 - \mathrm{Ext}_1) \times 3.22 = \mathrm{laminaran}\left(\mathrm{mg\ mL}^{-1}\right)$$

The mannitol content was estimated by periodate oxidation of the hexitol, according to the methodology described by Kremer (1981). The samples (10–20 mg dry material) were incubated in 2.5 mL methanol (80 %) at 70 °C for 1 h and centrifuged at 3500×$g$ for 15 min. The reaction was recorded at 260 nm in a scanning SUV-2120 spectrophotometer (SCINCO, Korea) and started by adding 1 mL aqueous (double-distilled water) methanol extract, to 1 mL 1 M acetate buffer (pH 4.5) and 1 mL Na-metaperiodate (3.5 mM). Readings were taken after 1 min and calibrated against a mannitol standard series (0–0.5 µmol mannitol $mL^{-1}$).

### Extraction and quantification of phlorotannins

Soluble phlorotannins were extracted from 10 mg of frozen material using acetone (70 %) as solvent and the Folin–Ciocalteu reagent as described by Koivikko et al. (2005) with modifications of algal weight, extract volumes and incubation times for 96-well plate (Cruces et al. 2012). The insoluble phlorotannins (the cell wall-bound fraction) were quantified according to the methodologies described by Strack et al. (1989) and modified by Koivikko et al. (2005). The content of phlorotannins in the extracts of soluble and cell wall-bound phlorotannins was determined using phloroglucinol (Sigma) as a standard. Based on calibration curves, the phlorotannin contents were expressed in dry weight units.

### Exposure to UV radiation

To study the impact of UV radiation on photosynthesis and concentration of soluble phlorotannins the disks were incubated under two irradiation conditions using lamps emitting PAR (TL Phillips), as well as UV-A (315–400 nm) and UV-B (280–315 nm) radiation (Q-panel 340 and Q-Panel 313, USA). In order to set two different UV treatments, the dishes were covered with different cutoff filters: a) PAR + UV-A + UV-B = Ultraphan 295 (Digefra, Germany), for exposure to full irradiance spectrum, and b) PAR = Ultraphan 395 (Digefra, Germany), which cut off all UV wavelengths.

Irradiances under the different combinations of lamps and cutoff filters were 2.4 and 8.8 $Wm^{-2}$ for UV-B and UV-A, respectively, while PAR was 125 µmol $m^{-2}$ $s^{-1}$. With respect to UV-B the exposure level is in the range of cloudless summer days at this latitude (Huovinen et al. 2006). The spectral characteristics of the lamps and filters are described by Cruces et al. (2013). The experimental irradiances were weighted using the action spectrum for photoinhibition of photosynthesis of isolated chloroplasts as normalized to unity at 300 nm (Jones and Kok 1966). The samples were exposed for different time periods (2, 6, 12, 24 and 48 h). At each time point, sample disks were taken for chlorophyll fluorescence measurements ($F_v/F_m$) and analyses of soluble phlorotannins.

The effects of UV radiation along the blades were measured as changes in maximal quantum yield of fluorescence ($F_v/F_m$) after a preincubation period (10–15 min) in the darkness using a PAM 2000 fluorometer (Walz, Effeltrich, Germany). The $F_v/F_m$ parameter is regarded as an indicator of the maximum quantum efficiency, where $F_v$ is the difference between the maximal fluorescence from fully reduced (closed) PSII reaction centers ($F_m$) and the initial fluorescence ($F_0$) from the antenna system of fully oxidized (open) PSII (Schreiber et al. 1994). The inhibition of

**Table 1** Longitudinal distribution PSII fluorescence kinetics from Imaging-PAM records

| Blade part | PSII quantum yield | | | P–E curve parameters | | |
|---|---|---|---|---|---|---|
| | $\Phi_{PSII}$ | $F_{m'}$ | NPQ | $ETR_{max}$ | $\alpha$ | $E_k$ |
| Blade 1 | | | | | | |
| Basal (1–4) | 0.675 ± 0.006 ab | 0.536 ± 0.036 d | 2.719 ± 0.370 bc | 16.489 ± 3.158 ab | 0.288 ± 0.078 | 60.124 ± 17.333 bc |
| Middle 1 (5–8) | 0.667 ± 0.011 a | 0.478 ± 0.015 c | 3.121 ± 0.118 c | 12.289 ± 0.877 a | 0.321 ± 0.009 | 38.338 ± 2.396 a |
| Middle 2 (9–2) | 0.678 ± 0.006 ab | 0.507 ± 0.027 d | 2.969 ± 0.115 c | 15.683 ± 0.600 ab | 0.313 ± 0.034 | 50.642 ± 6.066 b |
| Distal (10–15) | 0.676 ± 0.005 ab | 0.400 ± 0.216 ab | 3.017 ± 0.157 c | 15.463 ± 2.184 ab | 0.337 ± 0.029 | 46.307 ± 8.961ab |
| Blade 2 | | | | | | |
| Basal (1–3) | 0.696 ± 0.020 c | 0.510 ± 0.035 cd | 1.795 ± 0.965 ab | 20.891 ± 1.185 c | 0.327 ± 0.021 | 64.251 ± 7.236 c |
| Middle 1 (4–6) | 0.696 ± 0.002 c | 0.440 ± 0.025 b | 2.463 ± 0.025 b | 20.364 ± 0.755 c | 0.333 ± 0.006 | 61.338 ± 2.942 bc |
| Middle 2 (7–9) | 0.694 ± 0.001 b | 0.493 ± 0.012 c | 2.683 ± 1.345 bc | 19.571 ± 0.934 bc | 0.323 ± 0.015 | 60.706 ± 5.671 bc |
| Distal (10–12) | 0.695 ± 0.002 b | 0.409 ± 0.033 ab | 2.599 ± 1.307 bc | 19.837 ± 1.035 bc | 0.313 ± 0.025 | 63.720 ± 8.055 bc |
| Blade 3 | | | | | | |
| Basal (1–4) | 0.660 ± 0.007 a | 0.541 ± 0.013 d | 1.412 ± 0.225 a | 17.666 ± 1.796 bc | 0.282 ± 0.033 | 62.853 ± 1.610 bc |
| Middle 1 (5–8) | 0.672 ± 0.005 a | 0.381 ± 0.088 a | 1.600 ± 0.229 a | 21.255 ± 0.755 bc | 0.363 ± 0.041 | 59.902 ± 7.148 bc |
| Middle 2 (9–12) | 0.669 ± 0.002 a | 0.491 ± 0.020 c | 1.944 ± 0.241 a | 20.181 ± 1.054 bc | 0.333 ± 0.048 | 61.324 ± 5.912 bc |
| Distal (13–16) | 0.674 ± 0.002 ab | 0.501 ± 0.047 bc | 2.276 ± 0.163 b | 17.967 ± 1.612 ab | 0.318 ± 0.040 | 57.193 ± 8.318 bc |

Values represent mean ± S.D. of three selected blades (see Fig. 2). Numbers in brackets indicate the measuring points used for average calculations. Letters denote significant differences of means according to the post hoc Tukey's LSD test

photosynthesis was calculated as the percentage decrease between the value of $F_v/F_m$ measured in the PAR + UV treatment and the value recorded in samples maintained under PAR.

### Statistical treatment

Longitudinal variation in physiological parameters was compared by one-way analysis of variance (ANOVA) followed by Tukey's HSD post hoc analysis when differences were detected (Statistica 7.0, StatSoft Inc. USA). MANOVA and Pearson's correlation coefficient were used to determine the relationship between the different variables along the longitudinal profile. For Imaging-PAM data ($\Phi_{PSII}$, $F_{m'}$, NPQ and ETR vs. light parameters) two-way ANOVAs were performed, in which blades and blade parts were regarded as the independent factors. Normal distribution and homogeneity of variances were examined using Shapiro–Wilk's and Levene's tests, respectively. The effect of UV radiation was assessed through repeated-measures analysis of variance (RM-ANOVA) to test for changes in inhibition of $F_v/F_m$ and soluble phlorotannins (percentage of control without UV) in four blade parts (apical, middle 1, middle 2 and basal) over time (within-subject factor: 6, 12, 24 and 48 h). The assumption of sphericity was assessed by applying the Mauchly test. The multivariate Wilk's test criteria were used to test whether sphericity was violated.

## Results

### Longitudinal profiles

The profiles of imaging fluorescence did not reveal marked differences in photosynthetic activity between basal and apical regions (Fig. 2; Table 1). Two-way ANOVA revealed that for some fluorescence parameters (e.g., $\Phi_{PSII}$, and $E_k$) differences between blades were significant (Table S1). In the case of maximum fluorescence ($F_{m'}$), NPQ and $ETR_{max}$, an interaction between blade and blade parts could be inferred (Table S1). In general, effective quantum yield ($\Phi_{PSII}$) did not vary along the blades (Table 1); however, in algae with well-developed meristematic zone (e.g., blade 2 and 3; Table 1) the non-photochemical quenching (NPQ) showed lower values in this region and hence a lower potential to dissipate excess energy in basal compared to non-meristematic parts (Table 1). In contrast, parameters based on ETR versus $E$ curves ($ETR_{max}$, $\alpha$ and $E_k$) did not vary along the blade (Table 1, Table S1).

The blades of *L. spicata* exhibited variation in light $^{14}C$ fixation, with values increasing from 4.6 µmol $^{14}C$ $g^{-1}$ DW in the basal region to 12.7 µmol $^{14}C$ $g^{-1}$ DW in the distal zone (Fig. 3a, Table 2). In contrast, LICF values were higher (1.4 µmol $^{14}C$ $g^{-1}$ DW) in the intercalary, meristematic region, than in distal zone (0.7 µmol $^{14}C$ $g^{-1}$ DW; Fig. 3a, Table 2).

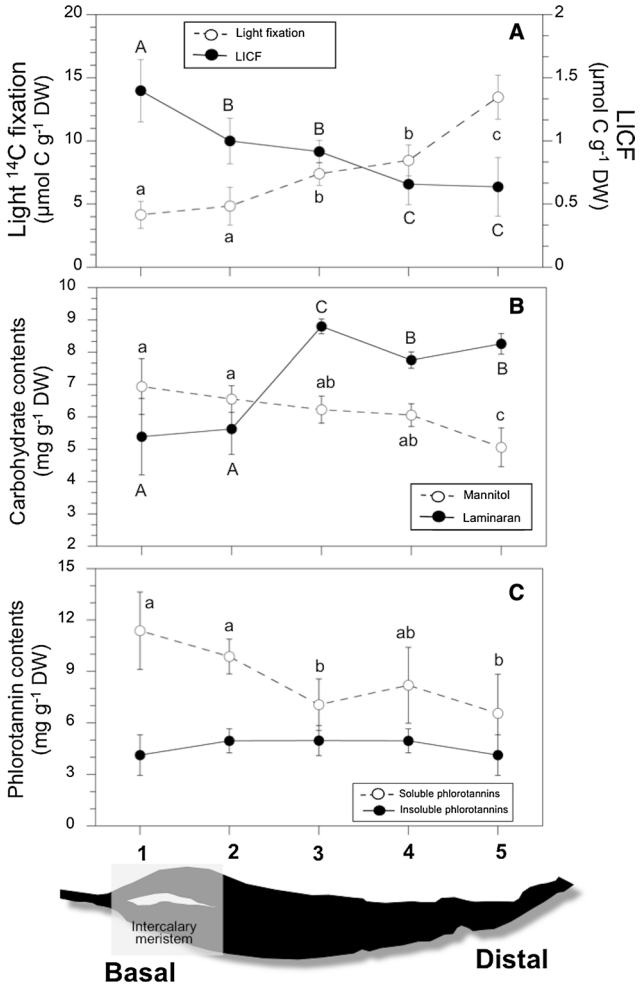


**Fig. 3** Longitudinal profiles along the blade of *Lessonia spicata*. **a** Photosynthetic $^{14}C$ fixation and light-independent $^{14}C$ fixation (LICF), **b** total content of mannitol and laminaran, **c** insoluble and soluble phlorotannins. *Numbers* indicate the location of punched blade disks for measurements and the shaded zone the location of the intercalary meristem. Values are mean ± S.D. (6 samples). *Letters* are results of post hoc Tukey's LSD test

Mannitol and laminaran contents were significantly different between the frond regions (Fig. 3b, Table 2). The compounds showed a reverse relationship with mannitol increasing toward the basal regions (6.9 mg $g^{-1}$ DW), while laminaran was the highest in the apical section (8.2 mg $g^{-1}$ DW) of the blades. The soluble phlorotannin content was higher in the basal than in the distal regions with values ranging between 6.5 and 11.4 mg $g^{-1}$ DW (Fig. 3c, Table 2). In contrast, the insoluble fraction varied less (4.1–4.9 mg $g^{-1}$ DW) increasing slightly toward the middle regions (Fig. 3c, Table 2). The MANOVA results indicated that the different physiological variables are affected by the intrinsic gradient in the blade and covariate (MANOVA, Wilk's test; Table 2). The Pearson correlation tests confirmed these patterns (Fig. 4): While soluble phlorotannins were negatively related to the longitudinal profiles of light $^{14}C$ fixation and the laminaran content, they showed a positive relationship with LICF and mannitol contents. Similarly, the longitudinal variation in laminaran and mannitol showed a positive relationship with light $^{14}C$ fixation and LICF, respectively (Fig. 4).

### Responses to UV radiation

UV exposures (PAR + UV-A + UV-B) caused a slight decline in chlorophyll fluorescence ($F_v/F_m$) (Fig. 5). After a 24-h UV exposure decreases in $F_v/F_m$ were >10 % of control in disks from all sections. Only after exposures for 48 h, chlorophyll fluorescence decreased significantly by 20 % (Fig. 5) and the RM-ANOVA revealed a significant interaction between time and blade parts (Table 3).

The contents in soluble phlorotannins (expressed as percentage of control) were affected by UV radiation over time (Fig. 6). After a 6-h UV exposure, the amount of phlorotannins decreased in disks from all blade sections between 35 and 46 %. After 12 h, phlorotannins were still low in disks from the middle and distal part (26 and 28 % less than control), while in those from the basal sections they increased. After 48 h the contents of soluble phlorotannins were stimulated by UV reaching values between 22 and 99 % of control (Fig. 6). The RM-ANOVA revealed that the phlorotannin concentration depended significantly on their allocation along the blade, the time of incubation and their interaction (Table 3).

## Discussion

This study showed that phlorotannin allocation along of blade of *L. spicata* is correlated with some physiological gradients related to growth, i.e., dark $^{14}C$ fixation and mannitol content. Moreover, phlorotannin content, but not chlorophyll fluorescence (as $F_v/F_m$), varied differentially between blade regions in response to UV radiation.

### Longitudinal profiles

The blades of *L. spicata* allocate only 25 % of the whole biomass of the adult individuals (holdfast diameter >20 cm). In contrast, structures involved in attachment and mechanical strength (holdfast and stipes) attain >70–75 % of the total allocated energy (Westermeier and Gómez 1996). However, blades are essential as they hold important processes such as growth and reproduction. In our study, photosynthetic $^{14}C$ fixation increased and LICF decreased from basal to distal parts of the blades, which is in agreement with the patterns described for blades of various kelps (Küppers and Kremer 1978; Gao and Umezaki

**Table 2** Results of one-way ANOVA and MANOVA for the variation of photosynthesis measured as $^{14}C$ fixation, light-independent carbon fixation (LICF) and different biochemical variables along the blade in *Lessonia spicata*

| Variable | *df* | SS | MS | *F* | *p* |
|---|---|---|---|---|---|
| $^{14}C$ light fixation | | | | | |
| Blade part | 4 | 213.72 | 53.432 | 31.778 | 0.00001 |
| Error | 14 | 25.539 | 1.681 | | |
| $^{14}C$ dark fixation (LICF) | | | | | |
| Blade part | 4 | 1.616 | 0.404 | 3.775 | 0.02564 |
| Error | 15 | 1.605 | 0.107 | | |
| Mannitol | | | | | |
| Blade part | 4 | 17.380 | 4.345 | 13.494 | 0.00001 |
| Error | 40 | 12.880 | 0.322 | | |
| Laminarin | | | | | |
| Blade part | 4 | 29.208 | 7.302 | 16.401 | 0.00023 |
| Error | 10 | 4.452 | 0.445 | | |
| Soluble phlorotannins | | | | | |
| Blade part | 4 | 131.264 | 32.816 | 8.135 | 0.00013 |
| Error | 31 | 125.043 | 4.034 | | |
| Insoluble phlorotannins | | | | | |
| Blade part | 4 | 4.363 | 1.091 | 1.053 | 0.40628 |
| Error | 19 | 19.674 | 1.035 | | |
| MANOVA (Wilk's test) | | | | | |
| Value = 0.00075<br>$F_{(24;\ 18)} = 5.316$<br>$p = 0.00025$ | | | | | |

1988). These patterns were also related to the profiles of storages carbohydrates, mannitol and laminaran as well as the contents in soluble phlorotannins (Figs. 3, 4). The high levels of photosynthetic $^{14}C$ fixation increasing toward the distal regions of *Lessonia* support well the prediction that middle and distal regions of the blades are constituted by well-developed tissues whose main function is synthesis of photoassimilates. In basal, meristematic tissues, which are mostly formed by tissues involved in anabolic processes, higher levels of LICF can be measured (Küppers and Kremer 1978). In fact, it has been demonstrated that carbohydrates such as laminaran are built in distal blade regions, which are then degraded with release of low molecular weight sugars (e.g., mannitol) (see Gómez and Huovinen 2012). During active growth, these compounds are translocated to the meristematic zone where they are converted to phosphoenol-pyruvate (PEP) to fuel, via LICF, the anaplerotic incorporation of $CO_2$ lost in glycolysis. Now, integrating the longitudinal patterns in phlorotannins contents, we can infer that high levels of soluble phlorotannins and mannitol in the basal–meristematic region of the fronds might be a functional strategy to power growth: mannitol as a source of energy to be used in glycolysis and phlorotannins as components in the formation of cell wall during enhanced cell division. It is known that soluble phlorotannins (the fraction sequestered in physodes) are precursors of the insoluble phlorotannins in the cell wall, where they act as complexing agents (Vreeland and Laetsch 1990). Thus, insoluble cell wall-bound phlorotannins have a structural function and their changes can be related to cell formation processes and response to environmental stress (e.g., UV radiation) (Schoenwaelder 2002). In *L. spicata,* the contents of insoluble phlorotannins did not vary along the blades challenging some predictions that state high soluble and low insoluble phlorotannins contents during active growth (Arnold 2003). Apparently, the levels of both fractions are not necessarily correlated, and in several species, the insoluble phlorotannins are non-inducible and always exhibit lower concentrations than the soluble fraction (Koivikko et al. 2005; Cruces et al. 2012; Gómez and Huovinen 2015).

High contents in phlorotannins in meristematic regions have been reported for various kelp species, e.g., *Eisenia arborea*, *Agarum fimbriatum*, *Laminaria complanata*, *L. farlowii* and *L. sinclairii*, while in other species such as *Egregia menziesii*, *Alaria marginata* and *Costria costata*, no obvious differences with non-meristematic tissues could be demonstrated (Van Alstyne et al. 1999). In some perennial *Laminaria* species, difference between new and old meristematic tissues has been found: Less phlorotannins were present in new as compared to older meristematic regions, outlining differences in functionality (e.g., grazing

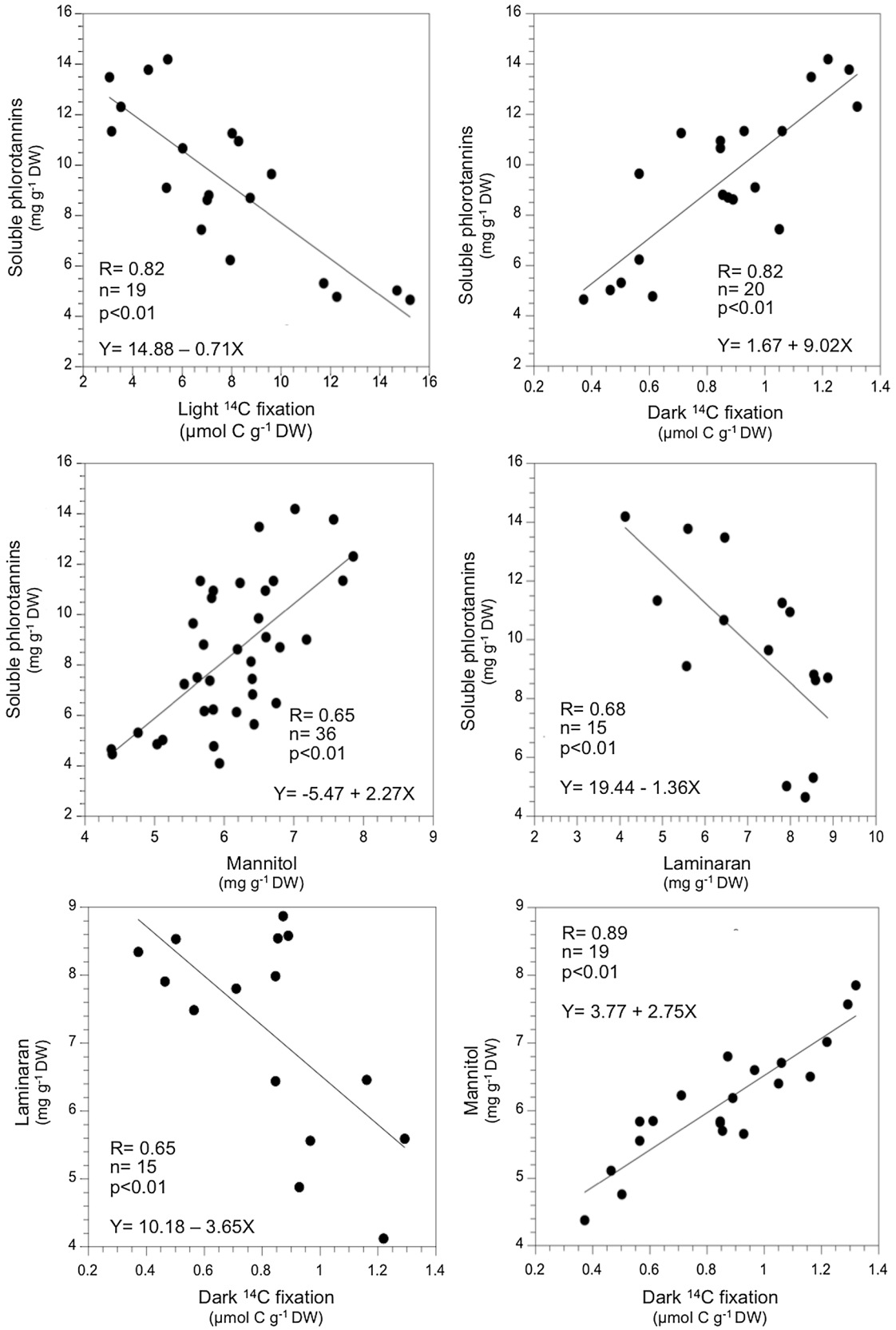


**Fig. 4** Relationship between the contents of soluble phlorotannins, $^{14}C$ fixation rates and contents of storage carbohydrates (mannitol and laminaran) measured along the blade in *L. spicata*. Linear equations, Pearson's coefficients (*R*), number of pairs (*n*) and significances are indicated

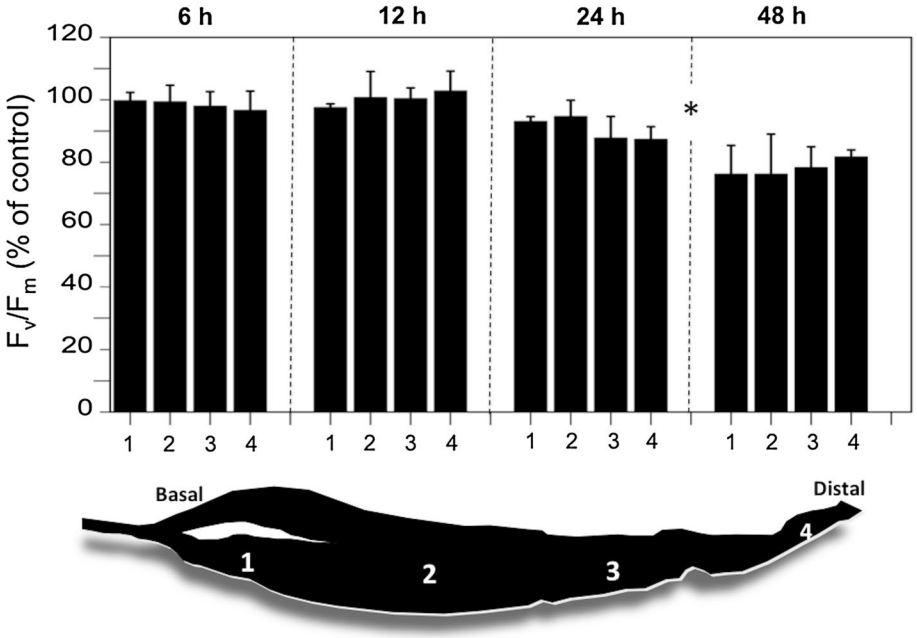


**Fig. 5** Effect of UV exposure for 48 h on the maximum quantum yield of fluorescence ($F_v/F_m$) measured on disks from different parts of the blade of *Lessonia spicata*. Values represent percentages of control (disks exposed to PAR). *Numbers* indicate the location of punched disks. Values are mean ± S.D. (6–8 samples). *Asterisk* denotes significant differences between time intervals ($p < 0.05$)

**Table 3** Results of repeated-measures ANOVA and multivariate analysis on the variation of $F_v/F_m$ (% of control) and soluble phlorotannins (% of control) along the blade of *Lessonia spicata* in response to UV exposure

| Variable | *df* | SS | MS | *F* | *p* |
|---|---|---|---|---|---|
| % Inhibition $F_v/F_m$ | | | | | |
| Blade part | 3 | 143.2 | 47.7 | 0.76 | 0.53301 |
| Error | 12 | 744.6 | 62.0 | | |
| Time | 3 | 5171.1 | 1723.7 | 58.41 | 0.00001 |
| Time × blade part | 9 | 607.8 | 67.5 | 2.28 | 0.03788 |
| Error | 36 | 1062.5 | 29.5 | | |
| Phlorotannin contents (%) | | | | | |
| Blade part | 3 | 22727.8 | 7575.9 | 23.958 | 0.00002 |
| Error | 8 | 2529.8 | 316.2 | | |
| Time | 3 | 84573.1 | 28191.0 | 196.43 | 0.00001 |
| Time × blade part | 9 | 27236.5 | 3026.3 | 21.087 | 0.00001 |
| Error | 24 | 3444.3 | 143.5 | | |

| Effect | Test | Value | *F* | Effect/error *df* | *p* |
|---|---|---|---|---|---|
| *Multivariate analysis* | | | | | |
| % Inhibition $F_v/F_m$ | | | | | |
| Time | Wilk's | 0.06 | 48.49 | 3/10 | 0.00001 |
| Time × blade part | Wilk's | 0.19 | 2.61 | 9/24 | 0.02846 |
| Phlorotannin contents (%) | | | | | |
| Time | Wilk's | 0.008 | 226.109 | 3/6 | 0.00001 |
| Time × blade part | Wilk's | 0.002 | 18.563 | 9/14 | 0.00002 |

| Effect | W | $\chi^2$ | *df* | *p* |
|---|---|---|---|---|
| *Mauchly sphericity test* | | | | |
| % Inhibition $F_v/F_m$ | | | | |
| Time | 0.591 | 5.648 | 5 | 0.341 |
| Phlorotannin contents (%) | | | | |
| Time | 0.244 | 9.460 | 5 | 0.009 |

Results of Mauchly test for sphericity are also indicated

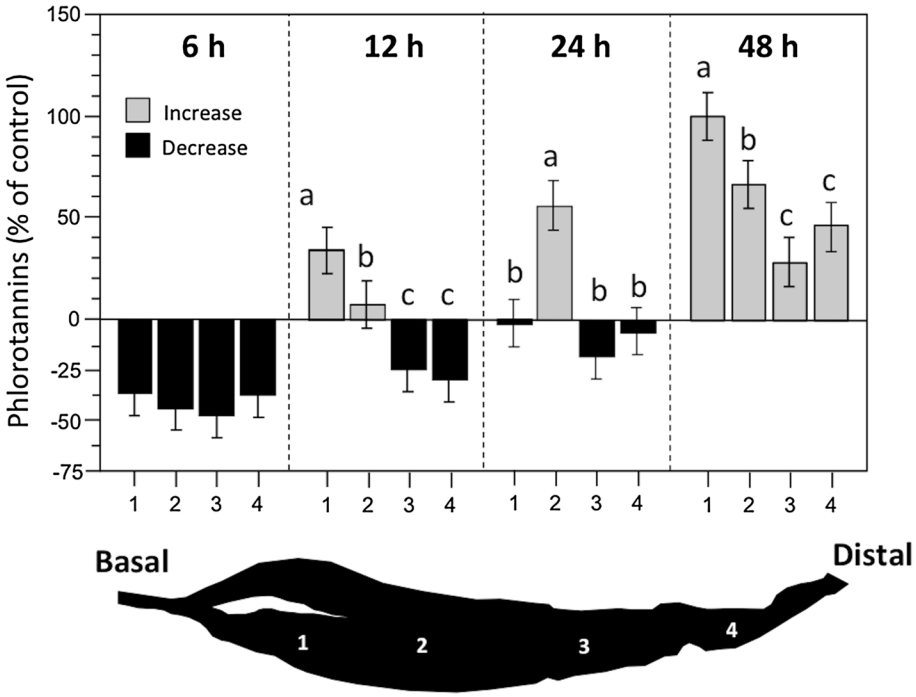


**Fig. 6** Effect of UV exposure for 48 h on the soluble phlorotannin contents measured on disks from different parts of the blades of *Lessonia spicata*. Values represent percentages in relation with control (disks exposed to PAR). *Numbers* indicate the location of punched disks. Values are mean ± S.D. (6–8 samples). *Different letters* denote significant mean differences within each exposure time according to post hoc Tukey's LSD test

deterrence) of these compounds along the blade (Connan et al. 2006). In virtue of their multiple functions in the cell (Pavia et al. 1997; Schoenwaelder 2002; Cruces et al. 2012), the synthesis and accumulation of phlorotannins in a given blade part do not necessarily correlate with a single metabolic process. Probably, in these brown algae characterized by large size, complex morphology and perennial development, a trade-off between biomass formation, reproduction and endurance against physical and biological factors is operating. For example, in *L. spicata*, synthesis of phlorotannins is stimulated during summer when photoprotection due to enhanced solar radiation and active growth (formation of cell wall) is required simultaneously (Gómez and Huovinen 2010).

In contrast to $^{14}C$ fixation, longitudinal patterns in chlorophyll fluorescence-based photochemical kinetics were less evident. Only in blades with marked differentiation of meristematic zone (e.g., blades 2 and 3) Imaging-PAM fluorescence parameters such as $F_{m'}$ and NPQ varied between blade parts (Table 1; Table S1). Interestingly, the low NPQ determined in basal, meristematic parts of blades 2 and 3 suggests that these tissues have less developed mechanisms for dissipation excess energy than middle and apical parts. Although the ultrastructural organization along the blade did not change greatly, it could be that the new cells arising from the activity of the meristem are in an initial phase of acquisition of their suite of PSII energy-dependent quenching mechanisms (Šesták 1985). Similarly, basal–meristematic sections of the blades had lower rates of photosynthetic $^{14}C$ fixation than middle and distal regions. When different thallus parts of *L. spicata* (blades, stipes and holdfast) are examined, marked differences in the fluorescence kinetics have been reported: Blades and stipes show highest $ETR_{max}$ values and saturating light requirements ($E_k$) compared to the holdfast (Gómez et al. 2005). The discrepancies between quantum yield of fluorescence ($\Phi_{PSII}$), and hence ETR estimations, with quantum yield of $CO_2$ fixation-related kinetics have been commonly discussed and point to that both processes can be affected by different electron sink (e.g., photorespiration or the Mehler reactions) (Hartig et al. 1998; Baker 2008). However, when photorespiration is inhibited, e.g., by lowering atmospheric oxygen from 21 to 2 % and $CO_2$ assimilation is the only major sink for NADPH and ATP, a linear relationship exists between photochemistry and $CO_2$ fixation efficiencies (Baker 2008).

## Responses to UV radiation

$F_v/F_m$ decreased with time of UV exposure, however, with no variation along the blades. Moreover, UV exposure after 48 h reduced inhibition of $F_v/F_m$ only by 22 %, which agrees with previous studies that characterize this species as UV stress tolerant, at least at short term (Gómez et al. 2007; Cruces et al. 2012). These results may be related to the invariable levels of insoluble, cell wall-bound phlorotannins along the blade (Fig. 2c), as this fraction has been related to the structural UV shielding in *L. spicata*, ameliorating the UV impact on photochemistry and key molecules (Gómez and Huovinen 2010). Alternatively, the

whole blade of *L. spicata* shows efficient photochemical mechanisms to quench excess energy, e.g., PAR-mediated photoinhibition, and enhanced non-photochemical quenching. It must be emphasized that in the present study, photoinhibition by PAR was not evaluated; however, it has been reported that this species shows a well-developed down regulation of photosynthesis when is exposed to natural solar radiation. For example, dynamic photoinhibition measured as a decrease in $F_v/F_m$ was close to 67 % at the noon (max PAR irradiances close to 2300 μmol $m^{-2}$ $s^{-1}$), and recover by 80–90 % in the afternoon (Cruces et al. 2013).

In contrast to photochemistry, soluble phlorotannin contents from different blade parts showed distinct responses to UV exposure: After 12- and 48-h exposure, phlorotannins measured in the basal (meristematic) region were significantly higher than in middle and apical regions. Although after 6-h exposure phlorotannins decreased with respect to control, the UV exposure for 12, 24 and 48 h overall stimulated the accumulation of soluble phlorotannins, pattern previously reported in this species (Gómez and Huovinen 2010). These results point to a UV acclimation of this species, which involves different levels of responses: rapid photochemical adjustments during the first hours of exposure following by synthesis of antistress substances (in this case phlorotannins) increasing the antioxidant activity against reactive oxygen species (ROS) (Cruces et al. 2012). In fact, increased levels of phlorotannins in response to UV radiation have been closely correlated with enhanced ROS scavenging capacity in various temperate and sub-Antarctic kelps (Connan et al. 2007; Cruces et al. 2012; 2013). However, although high levels of phlorotannins can be regarded as a suitable proxy for the estimation of the ROS scavenging potential of a given species, it is not clear whether this relationship operates in the context of morpho-functional differentiation along the thallus. For example, Connan et al. (2006) demonstrated that high levels of phenolic compounds measured in some parts of the thallus (meristematic zones, haptera, etc.) were correlated with an enhanced antioxidant activity. These authors suggested that differential functionality of phlorotannins (e.g., due to changes in the pool composition) could explain some of the response found between thallus parts. There is evidence that different species of phlorotannins (e.g., phlorofucofuroeckol A, eckol, dieckol and 8,8-bieckol) exhibit higher antioxidant potential than others (Shibata et al. 2008). Similarly, fractions of the phlorotannin pool of *Fucus vesiculosus* extracted using, e.g., ethyl acetate and 1-butanol, showed high antioxidant activity comparable to well-known standard antioxidants (e.g., α-tocopherol and L-ascorbic acid), while the fraction extracted using *n*-hexane had significantly lower ROS scavenging capacity (Wang et al. 2012). Due to their structural complexity in terms of polymerization and molecular weight (Heffernan et al. 2015), the question how these compounds and their properties change in function of cellular processes or in response to environmental variation remains unanswered.

The optimal defense theory (ODT), which predicts that chemical defenses are allocated to thallus regions with high fitness value (Cronin 2001), has been invoked to demonstrate that high contents of phlorotannins, e.g., in reproductive tissues, confer advantages for the overall fitness in scenarios of enhanced grazing (Yates and Peckol 1993; Steinberg 1995; Pansch et al. 2008) or high UV radiation (Huovinen and Gómez 2015). The ODT also suggests that chemical defenses are produced in direct proportion to the risk, i.e., the phenolic compounds would be produced at a direct expense of other functions (Pavia et al. 1999). High concentrations of phlorotannins may be expected when grazing pressure or UV radiation is high (inducible response), in thallus parts that make an important contribution to the whole fitness (e.g., meristematic or reproductive regions), which was confirmed in our study. On the other hand, production of phlorotannins has high costs and at the expense of growth rates (Pavia et al. 1999). Interestingly, costly defense systems favor inducible rather than constitutive defenses (Rhoades 1979), which has been confirmed in studies of simulated herbivory (Lüder and Clayton 2004) and under exposure to UV radiation (Gómez and Huovinen 2010). However, many brown algae, such as some species of *Fucus* (Creis et al. 2015) and various Antarctic Desmarestiales (Fairhead et al. 2006, Gómez and Huovinen 2015), do not show induction of phlorotannins in response to UV radiation, which suggests that these compounds are forming part of constitutive defenses. Apparently, algae with high concentrations (e.g., exceeding 20 mg $g^{-1}$ DW) normally do not exhibit UV induction of phlorotannins (Rautenberger et al. 2015).

In conclusion, our study confirmed the prediction that soluble phlorotannins are preferentially allocated to basal region where meristematic activity takes place. This pattern was correlated with higher rates of light-independent (dark) $^{14}C$ fixation (LICF) and high contents of mannitol, a carbohydrate normally used in anaplerotic processes. The second prediction, the longitudinal profiles in UV stress tolerance, was only partially corroborated: While soluble phlorotannins increased at the basal regions of the blade with increasing UV exposure time, maximum quantum yield ($F_v/F_m$), an indicator of efficiency of photochemistry under stress condition, did not vary along the blade. Overall, our results suggest that the synthesis and accumulation of phlorotannins in this species are regulated by morpho-functional processes related to photosynthesis, biomass formation and energy allocation.

**Acknowledgments** This study was supported by CONICYT—Chile (FONDECYT 1130582 to PH and FONDECYT 1030343 to IG). The authors thank Instituto de Histología, Universidad Austral de Chile, for providing facilities for scintillation counting. We thank V. Flores (Pontificia Universidad Católica de Chile) for TEM ultrastructural analysis. The helpful technical assistance of M. Oróstegui, C. Rosas, T. Pérez and A. González is gratefully acknowledged.

## References

Arnold TM (2003) To grow and defend: lack of trade-offs for brown algal phlorotannins. Oikos 100:406–408

Baker NR (2008) Chlorophyll fluorescence: a probe of photosynthesis in vivo. Ann Rev Plant Biol 59:89–113

Cabello-Pasini A, Alberte RS (1997) Seasonal patterns of photosynthesis and light-independent carbon fixation in marine macrophytes. J Phycol 33:321–329

Chapman ARO, Craigie JS (1978) Seasonal growth in *Laminaria longicruris*: relations with reserve carbohydrate storage and production. Mar Biol 46:209–213

Connan S, Delisle F, Deslandes E, Ar Gall E (2006) Intra-thallus phlorotannin content and antioxidant activity in Phaeophyceae of temperate waters. Bot Mar 49:39–46

Connan S, Deslandes E, Ar Gall E (2007) Influence of day–night and tidal cycles on phenol content and antioxidant capacity in three temperate intertidal brown seaweeds. J Exp Mar Biol Ecol 349:359–369

Creis E, Delage L, Charton S, Goulitquer S, Leblanc C, Potin P, Ar Gall E (2015) Constitutive or inducible protective mechanisms against UV-B radiation in the brown alga *Fucus vesiculosus*? A study of gene expression and phlorotannin content responses. PLoS ONE 10(6):e0128003

Cronin G (2001) Resource allocation in seaweed and marine invertebrates: chemical defense patterns in relation to defense theories. In: McClintock JB, Baker BJ (eds) Marine chemical ecology. CRC Press, Boca Raton, pp 325–353

Cruces E, Huovinen P, Gómez I (2012) Phlorotannin and antioxidant responses upon short-term exposure to UV radiation and elevated temperature in three South Pacific kelps. Photochem Photobiol 88:58–66

Cruces E, Huovinen P, Gómez I (2013) Interactive effects of UV radiation and enhanced temperature on photosynthesis, phlorotannin induction and antioxidant activities of two sub-Antarctic brown algae. Mar Biol 160:1–13

Drew EA, Hastings RM (1992) A year-round ecophysiological study of *Himantothallus grandifolius* (Desmarestiales, Phaeophyta) at Signy Island, Antarctica. Phycologia 31:262–277

Fairhead VA, Amsler CD, McClintock JB, Baker BJ (2006) Lack of defense or phlorotannin induction by UV radiation or mesograzers in *Desmarestia anceps* and *D. menziesii* (Phaeophyceae). J Phycol 42:1174–1183

Gao K, Umezaki I (1988) Comparative photosynthetic capacities of the leaves of upper and lower parts of *Sargassum* plants. Bot Mar 31:231–236

Gómez I, Huovinen P (2010) Induction of phlorotannins during UV exposure mitigates inhibition of photosynthesis and DNA damage in the kelp *Lessonia nigrescens*. Photochem Photobiol 86:1056–1063

Gómez I, Huovinen P (2012) Morphofunctionality of carbon metabolism in seaweeds. In: Wiencke C, Bischof K (eds) Recent advances in seaweed biology. Ecological studies. Springer, Berlin, pp 25–46

Gómez I, Huovinen P (2015) Lack of physiological depth patterns in conspecifics of endemic Antarctic brown algae: a trade-off between UV stress tolerance and shade adaptation? PLoS ONE 10(8):e0134440

Gómez I, Wiencke C (1998) Seasonal changes in C, N, and major organic compounds and their significance to morpho-functional processes in the endemic Antarctic brown alga *Ascoseira mirabilis*. Polar Biol 19:115–124

Gómez I, Ulloa N, Oróstegui M (2005) Morpho-functional patterns of photosynthesis and UV sensitivity in the kelp *Lessonia nigrescens* (Laminariales, Phaeophyta). Mar Biol 148:231–240

Gómez I, Oróstegui M, Huovinen P (2007) Morpho-functional patterns of photosynthesis in the South Pacific kelp *Lessonia nigrescens*: effects of UV radiation on $^{14}C$ fixation and primary photochemical reactions. J Phycol 43:55–64

González A, Beltrán J, Hiriart-Bertrand L, Flores V, de Reviers B, Correa JA, Santelices B (2012) Identification of cryptic species in the *Lessonia nigrescens* complex (Phaeophyceae, Laminariales). J Phycol 48:1153–1165

Gruber A, Roleda MY, Bartsch I, Hanelt D, Wiencke C (2011) Sporogenesis under ultraviolet radiation in *Laminaria digitata* (Phaeophyceae) reveals protection of photosensitive meiospores within soral tissue: physiological and anatomical evidence. J Phycol 47:603–614

Grzymski J, Johnsen G, Sakshaug E (1997) The significance of intracellular self-shading on the bio-optical properties of brown, red and green macroalgae. J Phycol 33:408–414

Hartig P, Wolfstein K, Lippemeir S, Colijin F (1998) Photosynthetic activity of natural microphytobenthos populations measured by fluorescence (PAM) and $^{14}C$-tracer methods: a comparison. Mar Ecol Progr Ser 166:53–62

Heffernan N, Brunton NP, Fitzgerald RJ, Smyth TJ (2015) Profiling of the molecular weight and structural isomer abundance of macroalgae-derived phlorotannins. Mar Drugs 13:509–528

Holzinger A, Di Piazza L, Lütz C, Roleda MY (2011) Sporogenic and vegetative tissues of *Saccharina latissima* (Laminariales, Phaeophyceae) exhibit distinctive sensitivity to experimentally enhanced ultraviolet radiation: photosynthetically active radiation ratio. Phycol Res 59:221–235

Huovinen P, Gómez I (2015) UV sensitivity of vegetative and reproductive tissues of two Antarctic macroalgae is related to differential allocation of phenolic substances. Photochem Photobiol 91:1382–1388

Huovinen P, Gómez I, Lovengreen C (2006) A five-year study of solar ultraviolet radiation in southern Chile (39°S): potential impact on physiology of coastal marine algae? Photochem Photobiol 82:515–522

Huovinen P, Leal P, Gómez I (2010) Impact of interaction of copper, nitrogen and UV radiation on the physiology of three south Pacific kelps. Mar Freshw Res 61:330–341

Jones LW, Kok B (1966) Photoinhibition of chloroplast reactions. 1. Kinetics and action spectrum. Plant Physiol 41:1037–1043

Jormalainen V, Honkanen T (2008) Macroalgal chemical defenses and their roles in structuring temperate marine communities. In: Amsler CD (ed) Algal chemical ecology. Springer, Berlin, pp 57–89

Klem K, Ač A, Holuba P, Kováč D, Špunda V, Robson TM, Urbana O (2012) Interactive effects of PAR and UV radiation on the physiology, morphology and leaf optical properties of two barley varieties. Environ Exp Bot 75:52–64

Kogame Y, Kawai H (1996) Development of the intercalary meristem in *Chorda filum* (Laminariales, Phaeophyceae) and other primitive Laminariales. Phycol Res 44:247–260

Koivikko R, Loponen J, Honkanen T, Jormalainen V (2005) Contents of cytoplasmic, cell-wall-bound and exuded phlorotannins in the brown alga *Fucus vesiculosus*, with implications on their ecological functions. J Chem Ecol 31:195–209

Kremer BP (1981) Aspects of carbon metabolism in marine macroalgae. Oceanogr Mar Biol Annu Rev 19:41–94

Kremer BP (1984) Carbohydrate reserve and dark carbon fixation in the brown macroalga, *Laminaria hyperborea*. J Plant Physiol 117:233–242

Krumhansl KA, Demes KW, Carrington E, Harley CDG (2015) Divergent growth strategies between red algae and kelps influence biomechanical properties. Am J Bot 102:1938–1944

Küppers U, Kremer BP (1978) Longitudinal profiles of carbon dioxide fixation capacities in marine macroalgae. Plant Physiol 62:49–53

Lüder UH, Clayton MN (2004) Induction of phlorotannins in the brown macroalga *Ecklonia radiata* (Laminariales, Phaeophyta) in response to simulated herbivory—the first microscopic study. Planta 218:928–937

Lüning K, Schmitz K, Willenbrink J (1973) $CO_2$ fixation and translocation in benthic marine algae. III. Rates and ecological significance of translocation in *Laminaria hyperborea* and *L. saccharina*. Mar Biol 23:275–281

Meyer S, Louis J, Moise N, Piolot T, Baudin X, Cervic ZG (2009) Developmental changes in spatial distribution of in vivo fluorescence and epidermal UV absorbance over *Quercus petraea* leaves. Ann Bot 104:621–633

Pansch C, Gómez I, Rothäusler E, Véliz K, Thiel M (2008) Species-specific defense strategies of vegetative versus reproductive blades of the Pacific kelps *Lessonia nigrescens* and *Macrocystis integrifolia*. Mar Biol 155:51–62

Pavia H, Cervin G, Lindgren A, Åberg P (1997) Effects of UVB radiation and simulated herbivory on phlorotannins in the brown alga *Ascophyllum nodosum*. Mar Ecol Prog Ser 157:139–146

Pavia H, Toth G, Åberg P (1999) Trade-offs between phlorotannin production and annual growth in natural populations of the brown seaweed *Ascophyllum nodosum*. J Ecol 87:761–771

Ragan MA, Glombitza KW (1986) Phlorotannins, brown algal polyphenols. Prog Phycol Res 4:129–241

Rautenberger R, Huovinen P, Gómez I (2015) Effects of increased seawater temperature on UV tolerance of Antarctic marine macroalgae. Mar Biol 162:1087–1097

Rhoades DF (1979) Evolution of plant chemical defense against herbivores. In: Rosenthal GA, Janzen DH (eds) Herbivores: their interactions with secondary plant metabolites. Academic Press, New York, pp 3–54

Schmitz K (1981) Translocation. In: Lobban CS, Wynne MJ (eds) The biology of seaweeds. University of California Press, Berkeley, pp 534–558

Schoenwaelder MEA (2002) The occurrence and cellular significance of physodes in brown algae. Phycologia 41:125–139

Schreiber U, Bilger W, Neubauer C (1994) Chlorophyll fluorescence as a non-intrusive indicator for rapid assessment of in vivo photosynthesis. Ecol Stud 100:49–70

Šesták D (1985) Photosynthesis during leaf development. Springer, Netherlands

Shibata T, Ishimaru K, Kawaguchi S, Yoshikawa H, Hama Y (2008) Antioxidant activities of phlorotannins isolated from Japanese Laminariaceae. J Appl Phycol 20:705–711

Steinberg PD (1995) Seasonal variation in the relationship between growth rate and phlorotannin production in the kelp *Ecklonia radiata*. Oecologia 102:169–173

Strack D, Heileman J, Wray V, Dirks H (1989) Structures and accumulation patterns of soluble and insoluble phenolics from Norway spruce needles. Photochemistry 28:2071–2078

Swanson AK, Druehl LD (2002) Induction, exudation and the UV protective role of kelp phlorotannins. Aquat Biol 73:241–253

Swanson AK, Fox CH (2007) Altered kelp (Laminariales) phlorotannins and growth under elevated carbon dioxide and ultraviolet-B treatments influence associated intertidal food-webs. Glob Change Biol 13:1696–1709

Targett NM, Arnold TMJ (1998) Predicting the effects of brown algal phlorotannins on marine herbivores in tropical and temperate oceans. J Phycol 34:195–205

Van Alstyne KL, McCarthy JJ III, Hustead CL, Kearns LJ (1999) Phlorotannin allocation among tissues of northeastern Pacific kelps and rockweeds. J Phycol 35:483–492

Vreeland V, Laetsch WM (1990) A gelling carbohydrate in algal cell wall formation. In: Adair WS, Mecham RP (eds) Organization and assembly of plant and animal extracellular matrix. Academic Press, London, pp 137–171

Wang T, Jónsdóttir R, Liu H, Gu L, Kristinsson HG, Raghavan S, Ólafsdóttir G (2012) Antioxidant capacities of phlorotannins extracted from the brown algae *Fucus vesiculosus*. J Agric Food Chem 60:5874–5883

Westermeier R, Gómez I (1996) Biomass, energy contents and major organic compounds in the brown alga *Lessonia nigrescens* (Laminariales, Phaeophyceae) from Mehuín, south Chile. Bot Mar 39:553–559

Wiencke C, Gómez I, Dunton K (2009) Phenology and seasonal physiological performance of polar seaweeds. Bot Mar 52:585–592

Wikström SA, Pavia H (2004) Chemical settlement inhibition versus post-settlement mortality as explanation for differential fouling of two congeneric seaweeds. Oecologia 138:223–230

Wyka T, Robakowski P, Zytkowiak R (2008) Leaf age as a factor in anatomical and physiological acclimative responses of *Taxus baccata* L. needles to contrasting irradiance environments. Photosynth Res 95:87–99

Yates JL, Peckol P (1993) Effects of nutrient availability and herbivory on polyphenolics in the seaweed *Fucus vesiculosus*. Ecology 74:1757–1766